



# Amorphous phase separation in an Fe-based bulk metallic glass



Wei Guo<sup>a,b,\*</sup>, Pyuck-Pa Choi<sup>c</sup>, Jae-Bok Seol<sup>d,\*</sup>

<sup>a</sup> Center for Nanophase Materials Sciences, Oak Ridge National Laboratory, Oak Ridge, TN 37831, USA

<sup>b</sup> Max-Planck-Institut für Eisenforschung, Max-Planck-Straße 1, D-40237 Düsseldorf, Germany

<sup>c</sup> Department of Materials Science Engineering, KAIST, Daejeon 34141, South Korea

<sup>d</sup> National Institute for Nanomaterials Technology, POSTECH, Pohang 37673, South Korea

## ARTICLE INFO

### Article history:

Received 1 December 2016

Received in revised form 2 January 2017

Accepted 3 January 2017

Available online 4 January 2017

### Keywords:

Amorphous phase separation

Yttrium

Bulk metallic glass

Atom probe tomography

Glass forming ability

## ABSTRACT

Although lanthanide elements play a critical role in increasing the glass forming ability and mechanical property alternation of Fe based bulk metallic glass (Fe-BMG), the atomic scale configuration of lanthanide in Fe-BMG remained unexplored. Here we have studied atomic configuration in the amorphous state of as-cast 4 mm FeCoCrMoCBy bulk metallic glass sheet and its mechanical properties by nanoindentation, transmission electron microscopy, and atom probe tomography. The current results showed that yttrium rich clusters are enriched with carbon atoms in the amorphous state, and the three dimensional densities of these clusters can influence the hardness at the localized region. The finding of Y-C rich clusters also suggests that the amorphous phase separation can precede the devitrification process.

© 2017 Elsevier B.V. All rights reserved.

## 1. Introduction

Fe-based bulk metallic glasses (Fe-BMGs) have been widely used for engineering applications, such as corrosion resistant hard coatings and armor-piercing heads. The primary reasons for the use of Fe-BMGs are their high specific strength (strength to mass ratio), inexpensive use of major elements, and superior corrosion resistance [1–5]. Despite their promising potential as structural alloys, optimizing the glass forming ability (GFA) and further processing routes of these alloys are prerequisites. The addition of lanthanides, i.e. yttrium of 2 at.%, has allowed for increasing the GFA of Fe-BMGs from less than one mm to more than 12 mm as rod shape specimen during the drop casting process [6,7]. In addition, such microalloying strategy can dramatically change the plasticity and fracture energy of these alloys [8]. For example, in Fe<sub>49</sub>Cr<sub>15</sub>Mo<sub>14</sub>C<sub>15</sub>B<sub>6</sub> systems, the addition of lanthanides <2 at.% has reduced the Poisson's ratio and increased the ratio of the elastic shear modulus to the bulk modulus, leading to a tough to brittle transition for the material [8]. However, the chemical bonding environment of lanthanides (both metallic and covalent-like bonds), and its role in the enhanced GFA and varying the mechanical response are not clear. To this end, atom probe tomography (APT) is a versatile technique that can possess a detailed chemical configuration at the sub-nm scale.

It is therefore necessary to revisit the lanthanide-microalloyed Fe-BMGs for examining the atomic configuration at this stage.

The detailed chemical analysis at sub-nm scale may also help to uncover another open question: does phase separation precede the crystallization? To date, there is no clear scenario that if a phase decomposition can precede nanocrystallization, which is more favorable for crystallization [9]. For binary systems such as CuZr metallic glass, it is almost impossible to expect phase separation, because the constituents possess large negative heat of mixing, promoting the mixing of the constituents instead of separating them. However, for multicomponent alloys an overall driving force for decomposition may still exist. Knowing this scenario is very important to determine the time window for processing the BMGs between glass transition temperature and crystallization temperature, as discussed in previous studies [9]. In this work, the iron-based metallic glass former (Fe<sub>41</sub>Co<sub>7</sub>Cr<sub>15</sub>Mo<sub>14</sub>C<sub>15</sub>B<sub>6</sub>Y<sub>2</sub>, in at.%) was cast into 4 mm thick plate by adding 2 at.% Y. We performed correlatively transmission electron microscopy (TEM) and atom probe tomography (APT) not only to uncover the role of Y on GFA but also to answer the fundamental question of whether amorphous phase separation can precede nanocrystallization during the casting process.

## 2. Materials and methods

A Fe<sub>41</sub>Co<sub>7</sub>Cr<sub>15</sub>Mo<sub>14</sub>C<sub>15</sub>B<sub>6</sub>Y<sub>2</sub> alloy ingot was synthesized by arc melting high purity Fe (99.9%), Co(99.9%), Cr(99.9%), Mo(99.9%), C (99.9%), B(99.9%) and Y(99.9%), and then was cast into 4 mm thick

\* Corresponding authors at: Center for Nanophase Materials Sciences, Oak Ridge National Laboratory, Oak Ridge, TN 37831, USA (W. Guo).

E-mail addresses: [wguo2007@gmail.com](mailto:wguo2007@gmail.com) (W. Guo), [jb\\_seol@postech.ac.kr](mailto:jb_seol@postech.ac.kr) (J.-B. Seol).

plate. The crystal structure for the as-cast sample and isothermally annealed samples were examined by cobalt source X-ray generator. The TEM samples were prepared by mechanical polishing thin foils down to a thickness of less than 100  $\mu\text{m}$  and then polished by a twin-jet electropolishing in a solution of 1 part of HCl and 3.5 parts of methanol at the temperature of  $-31^\circ\text{C}$ .

The cross-section of Fe-BMGs was mechanically polished. The Hysitron Tribo750 indenter was then utilized for the nanohardness measurements, using a 50 nm Berkovich triangular pyramid indenter. Series of nanoindentation were performed from the surface to the center of the sample with an interval of 0.2 mm. At least 15 indentations were performed on each position to allow statistical analysis. The hardness of the bulk was measured using the continuous stiffness method at a constant strain rate  $\dot{P}/P = 0.05 \text{ s}^{-1}$ ; a holding segment of 10 s at maximum load of 4000  $\mu\text{N}$  was set before unloading.

Samples for APT measurements were prepared by electro-polishing followed by a treatment with a dual-beam focused ion beam (FIB) (FEI, Helios Nano-Lab 600) [10]. A LEAP (LEAP 3000X HR, CAMECA Instruments) was used to analyze the chemical inhomogeneity. Measurements were performed in the voltage mode. All of the measurements were performed at 30 K at  $<10^{-7}$  Pa pressure. The pulse fraction was 15%. The pulse repetition rate was 200 kHz at a detection rate of 0.005 atom per pulse. At least two or even more successful measurements were performed. The APT data sets were visualized using the IVAS software (version 3.6.8) by Cameca Instruments. Reconstruction of APT maps was calibrated by determining the radius and shank angle of APT tips.

After APT reconstruction, the autocorrelation function (ACF) is a versatile mathematical tool for quantifying the average spacing of the irregular nanoscale clusters, which is ideal for quantifying the phase separation in three dimensions. The 3D radial autocorrelation function,  $R_k$ , can be expressed as [11]:

$$R_k = \frac{1}{\sigma^2} \sum_{r=0}^{r_{\max}-k} (C_r - C_0)(C_{r+k} - C_0), \quad (1)$$

where  $C_r$  is the concentration of a spherical shell at radius  $r$  from the chosen center point,  $r_{\max}$  is the maximal radius over which the analysis is taken,  $\sigma^2$  is the variance of the compositions given by  $\sum_0^{r_{\max}} (C_r - C_0)^2$ , and  $C_0$  is the mean concentration of the element of interest. The first maximum peak represents the 3D spacing of the interested phase, which is the distance where the composition of element is most correlated with the central location.

### 3. Results and discussions

Fig. 1a shows the meso-scale morphology of as-cast Fe-BMGs with a thickness of 4 mm. It should be noted that the sample region at the surface of the BMG sheet experiences a higher cooling rate than that in the center ( $\sim 250 \text{ K s}^{-1}$  in difference), and hence can lead to different local chemical configuration and mechanical response. After a 15-indentation test measured at each position, the average hardness of Fe based BMG plates is shown in Fig. 1a. At the surface of these 4 mm Fe based BMG plates, the average

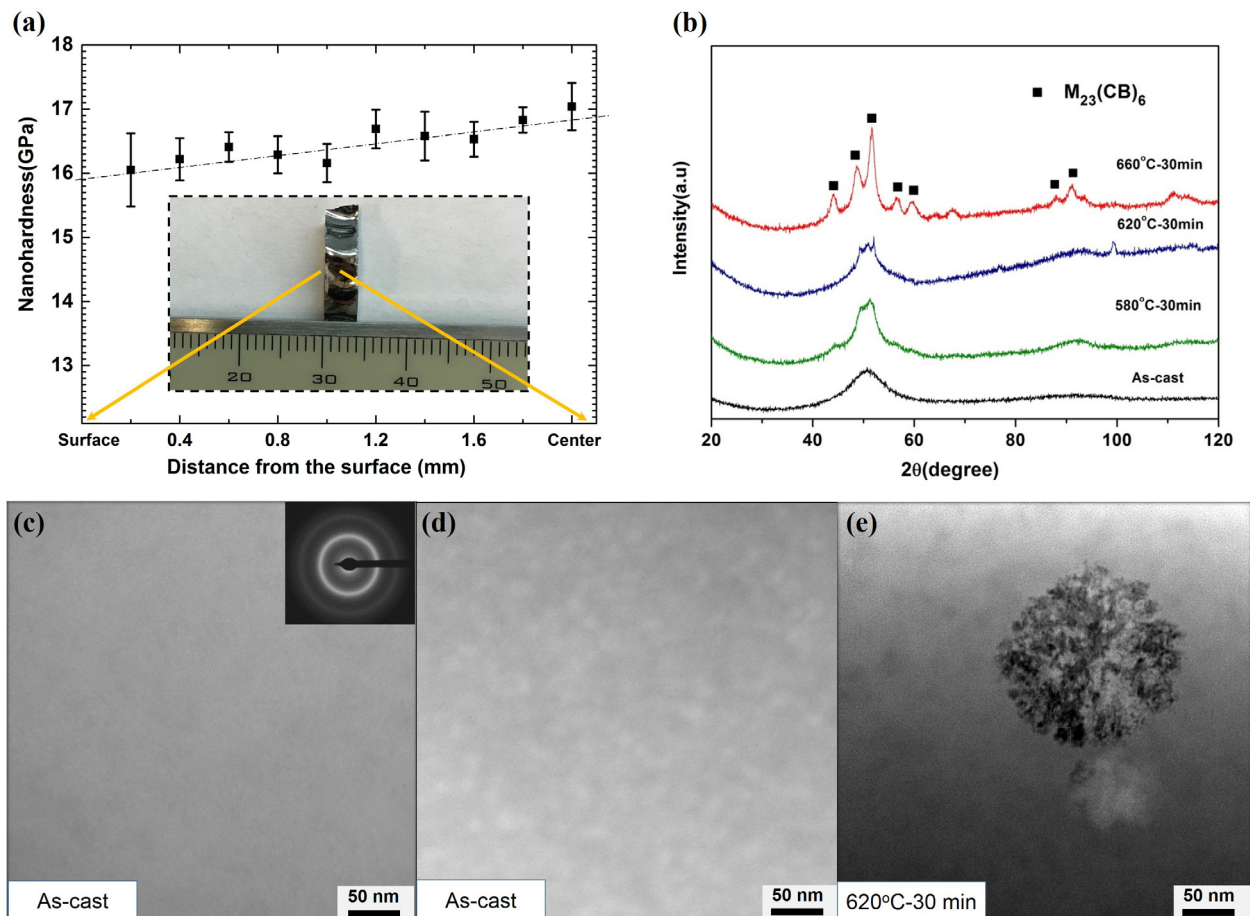


**Fig. 1.** Mechanical properties, crystallization routine, and microstructures of  $\text{Fe}_{41}\text{Co}_7\text{Cr}_{15}\text{Mo}_{14}\text{C}_{15}\text{B}_6\text{Y}_2$  as-cast bulk metallic glass: (a) Nanohardness profile across the thickness direction of 4 mm Fe-based bulk metallic glass; (b) X-ray diffraction of isothermal annealed samples revealed  $\text{M}_{23}(\text{CB})_6$  as the primary crystallization phase. (c,d) Representative bright field (BF) image (c) and HAADF image (d) taken at the surface of as-cast sample. (e) BF image of sample annealed at  $620^\circ\text{C}$  for 30 mins.

Download English Version:

<https://daneshyari.com/en/article/5464197>

Download Persian Version:

<https://daneshyari.com/article/5464197>

[Daneshyari.com](https://daneshyari.com)